

20TH CENTURY CLIMATE CHANGE IN THE TROPICAL ANDES: OBSERVATIONS AND MODEL RESULTS

MATHIAS VUILLE¹, RAYMOND S. BRADLEY¹, MARTIN WERNER² and
FRANK KEIMIG¹

¹*Climate System Research Center, Dept. of Geosciences, Morrill Science Center, Univ. of
Massachusetts, 611 North Pleasant Street, Amherst, MA 01003-9297, U.S.A.*

E-mail: mathias@geo.umass.edu

²*Max Planck Institute for Biogeochemistry, Jena, Germany*

Abstract. Linear trend analysis of observational data combined with model diagnostics from an atmospheric general circulation model are employed to search for potential mechanisms related to the observed glacier retreat in the tropical Andes between 1950 and 1998. Observational evidence indicates that changes in precipitation amount or cloud cover over the last decades are minor in most regions and are therefore rather unlikely to have caused the observed retreat. The only exception is in southern Peru and western Bolivia where there is a general tendency toward slightly drier conditions. Near-surface temperature on the other hand has increased significantly throughout most of the tropical Andes. The temperature increase varies markedly between the eastern and western Andean slopes with a much larger temperature increase to the west. Simulations with the ECHAM-4 model, forced with observed global sea surface temperatures (SST) realistically reproduce the observed warming trend as well as the spatial trend pattern. Model results further suggest that a significant fraction of the observed warming can be traced to a concurrent rise in SST in the equatorial Pacific and that the markedly different trends in cloud cover to the east and west of the Andes contributed to the weaker warming east of the Andes in the model. The observed increase in relative humidity, derived from CRU 05 data, is also apparent in the model simulations, but on a regional scale the results between model and observations vary significantly. It is argued that changes in temperature and humidity are the primary cause for the observed glacier retreat during the 2nd half of the 20th century in the tropical Andes.

1. Introduction

20th century climate change in the tropical Andes (Figure 1) is poorly documented because of inadequate spatial and temporal data coverage. The recession of tropical Andean glaciers throughout this century, however, indicates that such a change is indeed under way. In the tropical Andes of Peru 10 glaciers have been monitored since 1932, all retreating between 590 m and 1910 m through 1994 (Ames, 1998). Many of these glaciers may completely disappear within 50 years if current climatic conditions prevail (Brecher and Thompson, 1993; Hastenrath and Ames, 1995; Ames and Hastenrath, 1996; Francou et al., 2000; Ramirez et al., 2001). There is clear evidence that the glacier retreat has accelerated over the last two decades, as documented on the Qori Kalis glacier in Peru, where the rate of retreat



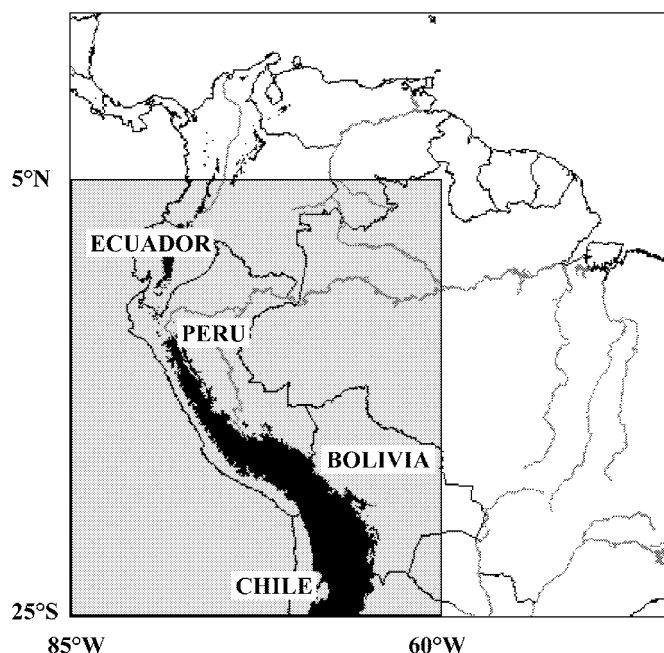


Figure 1. Location of the study area (5° N–25° S; 85° W–60° W). Dark shaded areas represent elevations >3000 m.

was nearly 3 times as fast between 1983 and 1991 (13.8 m yr^{-1}) as between 1963 and 1978 (4.9 m yr^{-1}) and the rate of volume loss was over seven times as great ($290,000 \text{ m}^3 \text{ yr}^{-1}$ as compared to $2,155,000 \text{ m}^3 \text{ yr}^{-1}$) (Brecher and Thompson, 1993). On the Antisana glacier in Ecuador mass balance measurements indicate an average negative mass balance of $600\text{--}700 \text{ mm yr}^{-1}$ during the last decade, and in Bolivia the Chacaltaya glacier lost 60% (93%) of its ice volume between 1940 and 1983 (1998) (Francou et al., 2000, 2003).

Since this evidence of glacier recession shows a very coherent pattern throughout the tropical Andes, it is reasonable to assume that it is associated with a large-scale climatic forcing, rather than caused by micro-climatic effects. In most instances this retreat has been attributed to a general warming of the tropical troposphere, leading to increased melting and a generally negative glacier mass balance (i.e., Thompson, 2000). Even though such a warming has recently been confirmed for the tropical Andes (Vuille and Bradley, 2000), and rising temperature may be the most likely candidate to explain the retreat over the last few decades (Kaser, 1999), glaciers may also suffer from a negative mass balance due to negative trends in precipitation and/or enhanced absorption of solar radiation due to a decrease in cloudiness. A decrease in precipitation and convective cloud cover, for instance, most likely led to a negative glacier mass balance and thus to the initial breakup of the ice cap on Mt. Kilimanjaro at the end of the last century (Hastenrath, 2001) and has also led to glacier retreat in the Cordillera Blanca, Peru

between 1930 and 1950 (Kaser and Georges, 1997). Besides changes in temperature, precipitation or cloud cover, a negative glacier mass balance may also be the result of an increased water vapor content leading to a change in sensible and latent heat transfer (Hastenrath and Kruss, 1992a,b). Energy balance studies on glaciers in Bolivia have shown that increased humidity in near surface levels, leading to a reduction of the vapor pressure difference between snow and air, will reduce sublimation but increase melt (Wagnon et al., 1999a,b). To sublimate snow, however, requires about 8 times as much energy as to melt it, so an increased humidity content in near surface levels will likely lead to higher overall ablation rates. This process is particularly important in dry environments such as the subtropical Andes (Kaser, 1999).

For all these parameters (cloud cover, precipitation, near-surface temperature and humidity), which influence the energy and mass balance of tropical glaciers, sufficient data are now available to attempt a first analysis of trends and step changes that might have occurred over the second half of this century, 1950–1994. In some cases we provide additional information for changes during the last two decades (1979–1998), because (a) this period is associated with an accelerated retreat of many Andean glaciers, (b) new satellite-derived products are available (e.g., OLR) and (c) it allows for a comparison with diagnostics from a new high-resolution Atmospheric General Circulation Model (AGCM) simulation. Using such model runs cannot replace the interpretation of observational data, but if model results and observations match, the models might provide additional information, which could help to attribute a particular change in climate to its causal mechanism.

In the next section we present the data we used in this study and the methods that we applied. In Section 3 we present the results of the trend analysis separately for convective activity and cloud cover, precipitation, temperature and relative humidity. In Section 4 we employ an AGCM to investigate the mechanisms that might have caused the observed climate change. Section 5 includes a discussion of the results and ends with some concluding remarks.

2. Data and Methods

The precipitation data was extracted from a database, which has in part already been presented by Vuille et al. (2000a,b). We used the 42 longest and most reliable records with monthly resolution for the time period 1950–1994 to analyze trends in precipitation. All data form part of the national meteorological networks in Ecuador, Peru, Bolivia, Chile and Argentina. All data had previously been error-checked and, if necessary, homogenized, as outlined in Vuille et al. (2000a,b). Besides checking all trends for statistical significance they were also analyzed for spatial coherence and elevation dependence.

The temperature analysis consists of an update of a recent study (Vuille and Bradley, 2000) and includes new data over southern and central Peru, now totaling 277 stations from 0 to 5000 m a.s.l. between 1° N and 23° S. Again all the data form part of the national meteorological networks, but unlike the precipitation data, many temperature records are short and cover only a few years. Rather than presenting individual station trends, we therefore chose to aggregate the data into one long time series (1950–1994) representative of the entire Andean range. We used the first difference method (Peterson et al., 1998), which allows the use of all available data without referencing it to a common base period. Because the Andes represent such a powerful divide for the lower-tropospheric flow separating the world's most arid desert (Atacama) to the west from the humid Amazon basin to the east, temperature trends were also analyzed as a function of elevation and the aspect of the slope. This was achieved by binning the data into 1000 m elevation zones and differentiating between the eastern and western slope below 2500 m. Only trends over the last 36 years (1959–1994) are presented for this analysis, because insufficient data were available for some elevation zones before 1959. In addition we use temperature data from the Climatic Research Unit (CRU) 05 data set (New et al., 2000). The data consists of monthly mean temperature interpolated from station records onto a global 0.5° latitude \times 0.5° longitude grid, covering land areas only. Although data are available starting in 1900, we only analyzed trends for the second half of this century (1950–1994), when the data is more reliable and to make the results comparable with the other analyses.

Several cloud cover data sets exist, which can be used to assess changes in cloud cover over the past decades. The International Satellite Cloud Climatology Project (ISCCP) contains the most comprehensive data set, but unfortunately it is not very well suited for linear trend analysis because of its short duration (start in July 1983) and the lack of an independent confirmation of the long-term calibration (e.g., Rossow and Schiffer, 1999). Highly reflective cloud (HRC) satellite data, is a good and frequently used proxy for convective cloud cover over the tropics (e.g., Waliser et al., 1993), but it does not take into account low- and mid-level cloud cover. Here we use monthly outgoing longwave radiation (OLR) data available since 1974 on a 2.5° latitude \times 2.5° longitude grid and corrected for potential biases due to differences in equator crossing times among the various polar orbiting satellites (Waliser and Zhou, 1997; Lucas et al., 2001). OLR is sensitive to the amount and height of clouds over a given region and time and has been applied in a number of studies to investigate tropical convection and convective cloud cover over tropical South America (e.g., Chu et al., 1994; Kousky and Kayano, 1994; Aceituno and Montecinos, 1997; Liebmann et al., 1998; Chen et al., 2001). In the presence of deep convective clouds, the satellite sensor measures radiation emitted from the top of the clouds, which are high in the atmosphere and thus cold, leading to low OLR values. In the case of clear sky conditions on the other hand, high OLR values reflect radiation emitted from the earth's surface and the lower atmosphere. In the absence of convective clouds, OLR is thus strongly influenced

by other processes, such as changes in surface temperature, low-level cloud cover or water vapor content (e.g., Waliser et al., 1993). We therefore only interpret trends in regions with a mean seasonal OLR value $<240 \text{ Wm}^{-2}$, a threshold often used to distinguish convective from non-convective regions, as a change in convective cloud cover (e.g., Morrissey, 1986). While this threshold does not allow an analysis in regions and at times when cloud cover is generally rare (e.g., sub-tropical Andes in JJA), it minimizes potential biases due to boundary layer processes in regions of low cloud coverage.

Changes in relative humidity between 1950 and 1994 were investigated using data from the Climatic Research Unit (CRU) 05 data set. Relative humidity (RH) was derived from the CRU05 vapor pressure (e) and temperature (T) data by using the standard formulas:

$$RH = \frac{e}{e_s} \quad (1)$$

$$e_s = 6.108 \exp \left(\frac{17.27T}{237.3 + T} \right) \text{ hPa}, \quad (2)$$

where e_s is the saturated vapor pressure. While temperature (T) is a primary variable, vapor pressure (e) is based on synthetic data using predictive relationships with primary variables if no station input is available (New et al., 2000). Considerable caution should thus be exercised when interpreting results based on this data alone.

All analyses were done separately for each season (DJF, MAM, JJA, SON), but in most cases only results for the annual mean and austral summer (DJF) and winter (JJA) are shown and discussed. We put special emphasis on the results from the wet season (DJF), because energy and mass balance studies on tropical Andean glaciers indicate that the major mass loss occurs during the wet season; that is, accumulation and ablation seasons tend to coincide (e.g., Ribstein et al., 1995; Wagnon et al., 1999a,b; Francou et al., 2000; Wagnon et al., 2001; Francou et al., 2003). Trends were computed using an ordinary least squares regression and tested against the null hypothesis that the trend is not significantly different from 0 at the 95%-confidence level (F-test). All significance levels are adjusted by reducing the degrees of freedom due to serial correlation (persistence) of the data (Weatherhead et al., 1998).

Once the main trends have been identified in the observational time series, we employ an AGCM to diagnose possible mechanisms that underlie the observed changes in Andean climate. We use the ECHAM-4 model, which is based on a hybrid sigma-pressure coordinate system and was run with triangular truncation at both wavenumbers 30 (T30 $\sim 3.75^\circ \text{ lat.} \times 3.75^\circ \text{ lon.}$) and 106 (T106 $\sim 1.1^\circ \text{ lat.} \times 1.1^\circ \text{ lon.}$), including 19 vertical layers from surface to 30 hPa. Both model experiments were run with modern boundary conditions and forced with observed global sea surface temperature (SST) fields (GISST 2.2, Global sea-Ice and Sea

Surface Temperature). While greenhouse gas concentrations were kept at a constant modern level in the T106 run, these levels were adjusted annually in the T30 experiment. The two simulations were run for an unequal length of time, which should be kept in mind when comparing output between the different simulations. ECHAM-4 T30 is the longer run, starting in 1903, but we limit our analysis to the period 1950–1994, for which the SST forcing is more reliable and the model performance can be evaluated more realistically using observational data. The ECHAM-4 T106 experiment only covers the last two decades, 1979–1998. The first year in both runs was discarded to avoid data problems with model equilibration during spin-up time. The model performance has been analyzed in great detail over both the tropical Americas and the tropical Andes (Vuille et al., 2003a,b). While both experiments realistically reproduce the mean state and the observed spatiotemporal variability of South American climate on interannual timescales, the rather coarse resolution of the T30 simulation is inadequate to resolve important spatial features over the high Andean terrain. We therefore limit our discussion of the T30 simulation to trends in temperature, which is spatially more coherent than the other variables. Clearly, these GCM runs are not designed to detect climate change in the tropical Andes, but they are helpful tools that can provide additional insight into possible forcing mechanisms associated with a changing climate. If the models are able to reproduce the trends as seen in the observational data, this would emphasize the crucial role of global or regional SST forcing on tropical Andean climate, since it is the only major forcing (besides greenhouse gas concentrations, adjusted annually in the T30 experiment) included in these simulations.

3. Observations

3.1. CLOUD COVER AND CONVECTION

Figure 2 shows the trend in OLR between 1979 and 1998 for the annual mean (Figure 2a), austral summer (DJF, Figure 2b) and austral winter (JJA, Figure 2c). The annual mean trend pattern (Figure 2a) reveals that OLR has decreased slightly north of approx. 10° S (henceforth referred to as inner tropics) indicating an increase in convective cloud cover. The trend however is weak, not surpassing 0.1 to $0.3 \text{ W m}^{-2} \text{ yr}^{-1}$, and not reaching statistical significance. The largest change (up to $0.55 \text{ W m}^{-2} \text{ yr}^{-1}$) has occurred during austral summer, DJF, when the OLR decrease is significant in some limited areas to the east of the Andes over the Amazon basin (Figure 2b). This observed slight increase in convective activity and cloud cover in the inner tropics is consistent with earlier studies over the Amazon basin reaching similar conclusions (e.g., Chu et al., 1994; Chen et al., 2001). South of 10° S (henceforth referred to as outer tropics) the trend is reversed, featuring an increase in OLR. This pattern however is more difficult to interpret because OLR in the outer tropics is only a good proxy for convective activity and cloud cover

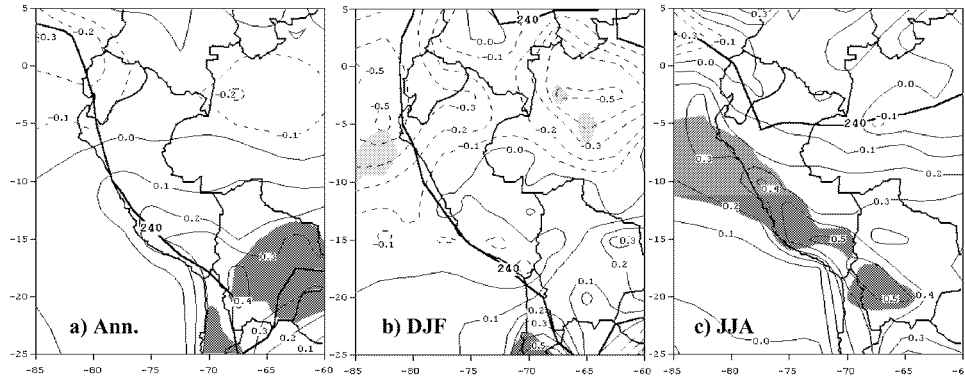


Figure 2. Trends in outgoing longwave radiation (ECT-corrected OLR). (a) Trend in annual mean OLR (1979–98), (b) as in (a) but for DJF, (c) as in (a) but for JJA. Contour interval is $0.1 \text{ W m}^{-2} \text{ yr}^{-1}$; negative contours are dashed. Thick black line indicates seasonal OLR threshold (240 W m^{-2}) to distinguish convective from non-convective regions. Regions where the trend is significantly increasing (decreasing) at the 95%-confidence level are shaded in dark (light) gray.

during the rainy season (DJF). There is indeed a slight increase in OLR in the outer tropics during DJF (Figure 2b), which may be indicative of reduced cloud cover and enhanced subsidence. This notion is consistent with results by Wielicki et al. (2002) and Chen et al. (2002) reporting intensified upward motion and cloudiness in equatorial-convective regions and drier and less cloudy conditions in subtropical subsidence regions in the 1990s, although questions have been raised about the reality of these variations (Trenberth, 2002). The larger fraction of this positive OLR trend in the outer tropics and along much of the Andean range, however, is a result of significant positive departures during the winter dry season (JJA, Figure 2c). At this time of the year, convective cloud cover is rare as indicated by the equatorward displacement of the 240 W m^{-2} threshold and OLR is sensitive to boundary layer processes, such as vapor content or surface temperature. The positive trend in OLR over the Andes in JJA therefore most likely does not or does not only reflect a change in convective cloud cover.

3.2. PRECIPITATION

Since OLR has been described as a good proxy for precipitation over tropical South America (i.e., Liebmann et al., 1998), it is worthwhile investigating whether the observed weak long-term changes in OLR are accompanied by contemporaneous trends in precipitation (e.g., Morrissey and Graham, 1996). Figure 3 shows this change (in mm yr^{-1}) as recorded by 42 stations in the tropical Andes between 1950 and 1994 (45 years). Overall there is little spatial coherence between the various station trends and no clear pattern of increasing or decreasing precipitation emerges. On the regional scale a weak tendency toward increased precipitation in northern Peru, between 5°S and 11°S for both the annual sum (Figure 3a) and the seasonal patterns (Figures 3b–c) emerges. In southern Peru and along the

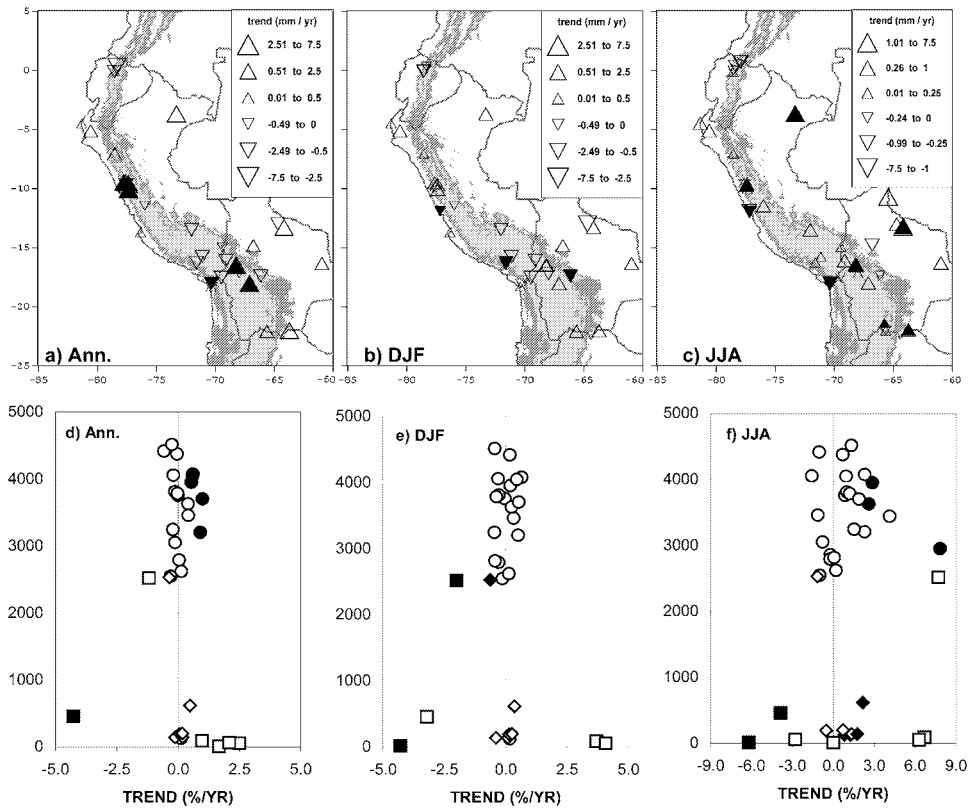


Figure 3. Trends in station precipitation (mm yr^{-1}) between 1950 and 1994 for (a) annual sum, (b) DJF, (c) JJA. Upward (downward) pointing triangles indicate an increase (decrease) in precipitation. Note different scaling in (c). Filled (open) triangles indicate that the trend is (not) significant at the 95%-confidence level. (d) As in (a) but trend in annual precipitation (in $\% \text{ yr}^{-1}$) versus elevation. (e) As in (d) but for DJF, (f) as in (d) but for JJA. Stations below ~ 2500 m are represented by squares (western slope) and diamonds (eastern slope); stations above 2500 are shown as circles. Trend shows change (in $\% \text{ yr}^{-1}$) compared to long-term mean (1950–1994) precipitation. Filled (open) symbols indicate that the trend is (not) significant at the 95%-confidence level.

Peru/Bolivia border most stations indicate a precipitation decrease for the annual total and during the main rainy season DJF (Figure 3b). In JJA most stations indicate an increase in precipitation, in particular the lowland stations to the east of the Andes and the Altiplano region of northern Bolivia and southern Peru (Figure 3c). Even in the case of a coherent regional signal however, individual station trends are mostly insignificant. Of the 42 stations analyzed only 5 (2) show a significant increase (decrease) in the annual precipitation amount. Furthermore one needs to take into account that several stations are located very close to one another and are thus not truly independent records, because they capture the same local climatic signal.

Since the precipitation amount varies with elevation, it is worthwhile to investigate whether the precipitation trend shows any signs of elevation dependence as well. In Figures 3d–f the trend in precipitation (in $\% \text{ yr}^{-1}$) is plotted versus elevation for the same 42 stations as in Figure 3a–c, with a subdivision into records from the eastern and western slope below 2500 m. No sign of elevation dependence is evident from Figure 3. Positive as well as negative trends occur at all elevations between 0 and 5000 m, although unfortunately stations in the 1000–2000 m elevation range are missing. The larger trends at lower elevations reflect the dry conditions of the Pacific coast where small changes in the absolute amount of rainfall lead to larger relative trends. During the JJA dry season there is a slight bias toward wetter conditions, with 27 (13) stations indicating a positive (negative trend), but no dependence on elevation is apparent.

3.3. TEMPERATURE

Figure 4a shows the annual mean temperature deviation from the 1961–1990 long-term mean in the tropical Andes between 1950 and 1994, based on 277 stations between 1° N and 23° S ranging from 0 m to 5000 m a.s.l. Temperature in the tropical Andes has increased by $0.15^\circ \text{ C decade}^{-1}$ since 1950. This long-term trend is superimposed on strong interannual variability associated with ENSO. Based on a very similar dataset Vuille and Bradley (2000) calculated a warming of 0.10 – $0.11^\circ \text{ C decade}^{-1}$ between 1939 and 1998 and of 0.32 – $0.34^\circ \text{ C decade}^{-1}$ between 1974 and 1998, indicating almost a tripling of the warming rate over the last 25 years.

The CRU05 data set, subsampled to match the location of station records used in Figure 4a, shows a very similar interannual variability, but a significantly lower overall warming trend of $0.09^\circ \text{ C decade}^{-1}$ (Figure 4b). When the trends are segmented into different elevation zones, based on 1000 m intervals with ± 500 m overlap, it becomes apparent that the lower warming trend in the CRU05 data is primarily due to a reduced warming along the western Andean slope (0.03 – $0.15^\circ \text{ C decade}^{-1}$, Figure 5b) when compared to the Vuille and Bradley (2000) data (0.21 – $0.37^\circ \text{ C decade}^{-1}$, Figure 5a). While the vertical bars in Figure 5 represent the 1000 m elevation zone for which the trend is valid, the horizontal bars indicate the 95% confidence limits for the trend and extend two standard errors of estimate on either side; that is, all trends whose horizontal bars do not intersect with the $0^\circ \text{ C decade}^{-1}$ trend abscissa are significant at the 95% level. The trends are generally higher and more significant in the Vuille and Bradley (2000) data (Figure 5a), but both data sets indicate a warming trend at all elevations, except on the eastern slopes, where the trend is insignificant (Vuille and Bradley, 2000, Figure 5a) or even negative (CRU05, Figure 5b) below 1000 m. Overall the lower elevations on the Pacific side have experienced the greatest warming while the temperature increase on the eastern slopes has been rather moderate. The higher elevations show a warming of approximately 0.05 – $0.20^\circ \text{ C decade}^{-1}$, with a warming trend

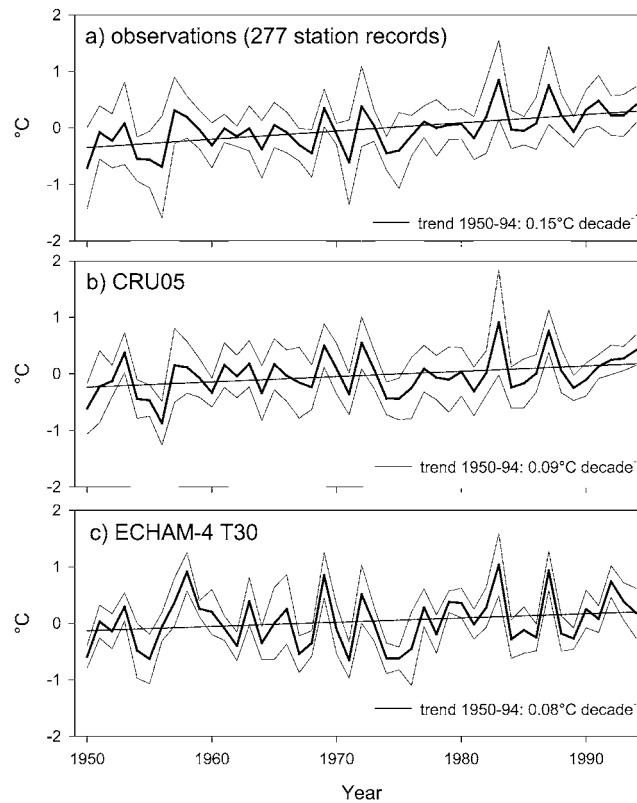


Figure 4. Temperature trend and annual departure from 1961–1990 average (\pm one standard deviation) in the tropical Andes ($\sim 1^{\circ}$ N– 23° S) between 1950 and 1994 based on (a) 277 station records (modified from Vuille and Bradley, 2000), (b) CRU05 data and (c) ECHAM-4 T30 simulation. Trends in (b) and (c) are based on sub-sampling of grid cells to match location of station records used in (a).

that is slightly decreasing with elevation above 3500 m in both data sets. This vertical structure of the temperature trend is different from what is observed in Tibet or the European Alps, where the warming is more pronounced at higher elevations. However, the high altitude warming in those regions is probably related to a decrease in spring snow cover, lower albedo values and a positive feedback on temperature (i.e., Liu and Chen, 2000). This mechanism is not as important in a tropical environment, where only a few mountain peaks reach above the 0°C isotherm at ~ 5000 m, and, due to the lack of thermal seasons, there is no ‘winter’ and ‘spring’ snow cover, which could influence the thermal regime in a way similar to that in the mid-latitudes (Kaser and Georges, 1999).

3.4. HUMIDITY

A significant increase in near-surface and tropospheric humidity over the last decades has been reported from both the eastern and western tropical Pacific

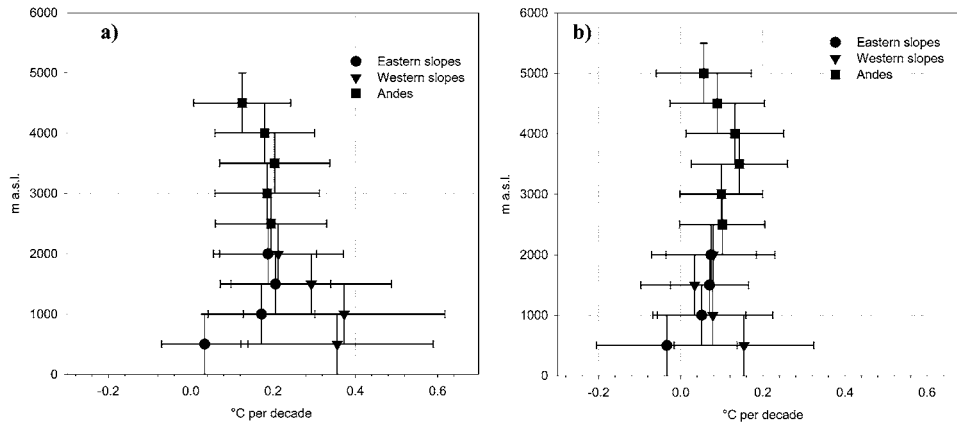


Figure 5. Mean annual temperature trend ($^{\circ}\text{C decade}^{-1}$) as a function of elevation (m a.s.l.) based on (a) observations (1959–1994, modified from Vuille and Bradley, 2000), (b) CRU05 (1959–1994). Vertical bars indicate elevation range (1000 m) for which trend is valid. Horizontal bars are 95% confidence limits for the trend (i.e., all trends whose error bars do not intersect with the $0^{\circ}\text{C decade}^{-1}$ abscissa are significant at the 95% confidence level). Results in (b) are based on sub-sampling to match station coverage in (a), that is only grid cells which contain station data in (a) are considered.

and tropical South America (Gutzler, 1992; Curtis and Hastenrath, 1999a,b) but changes over the tropical Andes have not been assessed so far. Here we present the change in relative humidity based on the CRU05 data set (New et al., 2000) between 1950 and 1994 (Figures 6a–c). In addition we also show trends for a short, more recent, time period (1979–1995, Figures 6d–f), which will be used to assess the model performance in Section 4.1. Changes over the last 45 years are most significant along the Andean range, featuring an increase in relative humidity between 0.0 and $2.5\% \text{ decade}^{-1}$, with the most prominent positive trend in northern Ecuador and southern Colombia, while in southern Peru, western Bolivia and northernmost Chile the increase is more moderate (0.5 – $1.0\% \text{ decade}^{-1}$). Overall the trends are very similar in all seasons with only slight modulations during winter and summer (Figures 6b–c). Given the significant increase in temperature and the rising relative humidity levels, it follows that vapor pressure (or specific humidity) has increased significantly throughout the Andes as well (not shown). To the east of the Andes the trends are much lower or even negative, especially during the last two decades (Figures 6d–f). During this more recent time period only the Andean range shows a positive trend, with a significant increase limited to central Peru (Figure 6d).

This decrease in relative humidity to the east of the Andes and over the western Amazon basin is hard to reconcile with the observed increase in convective activity (Figure 2) and is also in contradiction with other reports suggesting that humidity levels have increased in this region (e.g., Chen et al., 2001). Clearly caution should be exercised in the interpretation of the humidity trends shown in Figure 6 since the gridded CRU05 data over South America is partially interpolated from synthetic data (New et al., 2000). Nonetheless these results suggest that the near-surface

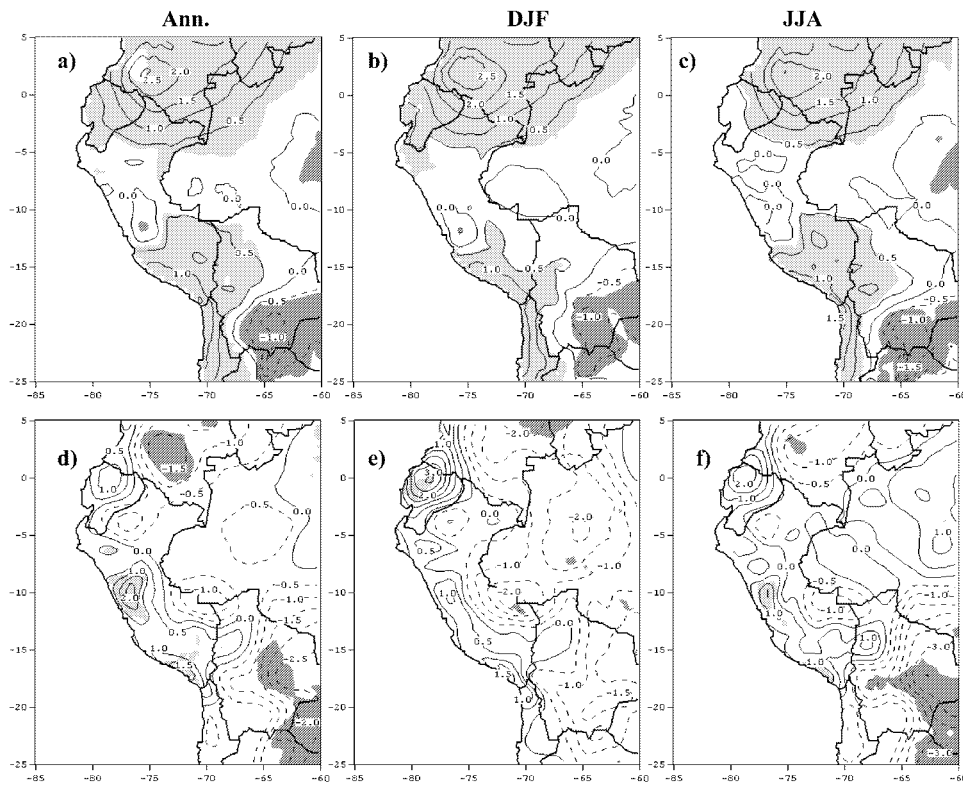


Figure 6. Trend in relative humidity (CRU 05) between 1950 and 1994 (top row) and 1979 and 1995 (bottom row) for annual average (left column), DJF (middle column) and JJA (right column). Contour lines are $0.5\% \text{ decade}^{-1}$; negative contours are dashed. Regions where the trend is significantly increasing (decreasing) at the 95%-confidence level are shaded in light (dark) gray. Figures have been smoothed with a 3×3 averaging filter.

moisture increase in the tropical Andes is not just due to rising temperatures but reflects an overall increase in both absolute and relative terms.

3.5. SUMMARY OF OBSERVATIONS

The observational evidence presented in the previous sections has revealed some significant changes in the surface climate of the tropical Andes over recent decades. OLR data indicates that convective cloud cover has increased slightly during DJF, especially in the inner tropics, while the significant positive OLR trends in JJA are difficult to interpret. The significance of the results is further limited by the short time series of available ECT-corrected OLR data, which in our analysis only covers 20 years (1979–1998). Nonetheless the trends in cloud cover are consistent with other reports of observed decrease in OLR over the Amazon basin (Chu et al., 1994; Chen et al., 2001) and are also in general accordance with the results from the precipitation analysis indicating a weak tendency toward increased precipitation

in northern Peru and a slight decrease in southern Peru. Overall the precipitation trends are weak, only a few stations meet the 95%-significance criteria, and the trends do not show any elevation-dependence. Furthermore the interpretation of the spatial pattern is somewhat hampered by the unequal distribution of the available station records.

Temperature shows an average warming of $0.09\text{--}0.15\text{ }^{\circ}\text{C decade}^{-1}$ between 1950 and 1994 with most of the warming taking place after the mid 1970s. The lower elevations to the west of the Andes have experienced the greatest warming, while the warming to the east is only moderate in the Vuille and Bradley (2000) data set and even negative in the CRU05 data set below 1000 m. The higher elevations show a warming which is higher than that on the eastern but lower than on the western slopes. The results are consistent with observations further to the north in the Andes of Colombia and Venezuela (Quintana-Gomez, 1999) and further to the south in the Andes of Chile (Rosenblüth et al., 1997), both reporting a warming of similar magnitude. An apparent discrepancy exists between our results, indicating a significant warming even at highest elevations between 4000 m and 5000 m, and the observed slight decrease in tropical freezing levels between 1979–1997 (Gaffen et al., 2000). Most likely these differences are real, indicating a differential warming of near-surface and free-air tropospheric temperatures at similar elevation. Whatever the cause for this difference may be, it shows the need for a dense surface observational network to monitor and detect climate change. Radiosonde and MSU data are clearly limited in their capacity to detect temperature trends at high elevation in the tropics.

Concurrent with the temperature increase, the relative humidity in near-surface levels has increased as well, by $0\text{--}2.5\% \text{ decade}^{-1}$ between 1950 and 1994. This increase in relative humidity shows that the absolute humidity increase is larger than what could be expected from a temperature increase alone.

The observed glacier retreat throughout the last decades in the tropical Andes has usually been related to increasing temperatures (i.e., Thompson, 2000). Given the fact that there has indeed been considerable warming over the last 5 decades even at the highest elevations, and that the increase has accelerated, concurrent with an enhanced retreat of the glaciers after the mid 1970s (Brecher and Thompson, 1993; Francou et al., 2000), this assumption seems reasonable. Higher temperatures also lead to a higher rain-snow line and glaciers will thus increasingly be exposed to rain in the ablation area. In addition our results suggest that increased humidity in near surface levels might have accelerated this retreat through increased melt rates. Caution should be exercised however in the interpretation of the humidity trends because the gridded CRU05 data over South America is partially interpolated from synthetic data (New et al., 2000). Long-term on-site observations of near-surface humidity are needed to confirm this notion of a positive humidity trend.

Changes in precipitation and cloud cover on the other hand can be ruled out with a high degree of confidence as major contributing factors. In the inner tropics the

cloud cover trend has clearly gone the other way and would favor a glacier advance. The positive OLR trend during the dry season on the other hand is probably less important because (a) cloud cover is minimal over the Andes at this time of the year, and (b) the major mass loss of tropical glaciers occurs during the wet season, DJF (e.g., Ribstein et al., 1995; Wagnon et al., 1999a,b, 2001; Francou et al., 2000, 2003). Precipitation amounts have changed little over the last 45 years, although there are several reports which indicate a precipitation increase on a regional scale to the east of the Andes, such as in Ecuador during the MAM rainy season (Vuille et al., 2000a), NW-Argentina (Villalba et al., 1998) or the lowlands of Bolivia (Ronchail, 1995). The only region where precipitation trends might have had a negative impact on glacier mass balance seems to be southern Peru, but even here the trends are weak and mostly insignificant.

4. Model Results

Since observations and CRU05 data indicate that changes in temperature and humidity are the most likely candidates to explain the current glacier retreat, we focus on these two variables in the next section. We employ the ECHAM-4 AGCM to investigate the following questions: First we test whether the model is capable of simulating the observed increase in temperature and humidity as well as the markedly differing temperature trends to the east and the west of the Andes (Section 4.1). If this is the case we will then search for potential mechanisms, which could explain this differential warming as well as the simulated overall temperature and humidity increase in the tropical Andes (Section 4.2).

4.1. TEMPERATURE AND HUMIDITY SIMULATION

Figure 4c shows the simulated interannual variability and long-term trend of air temperature in the tropical Andes as simulated by the ECHAM-4 T30 model between 1950 and 1994. To facilitate the comparison with the Vuille and Bradley (2000) (Figure 4a) and the CRU05 (Figure 4b) time series, the simulated temperature in Figure 4c was averaged over grid cells subsampled to match the location of stations used in Figure 4a. Clearly the interannual variability is very similar between observations and model, with El Niño (La Niña) years standing out prominently as warm (cold) anomalies. The overall warming trend is comparable to the CRU05 trend but significantly lower than in the Vuille and Bradley (2000) data.

The markedly different warming to the east and the west of the Andes is also reproduced in the ECHAM model (Figures 7a,b). The T30 (1950–1994) simulation (Figure 7a) shows the strongest warming to the west of the Andes along the Pacific coast ($0.1\text{--}0.15\text{ }^{\circ}\text{C decade}^{-1}$), and an insignificant warming or even a cooling ($-0.05\text{--}+0.05\text{ }^{\circ}\text{C decade}^{-1}$) to the east, consistent with the observational evidence. The much shorter experiment at T106 resolution (1979–1998) also reproduces the

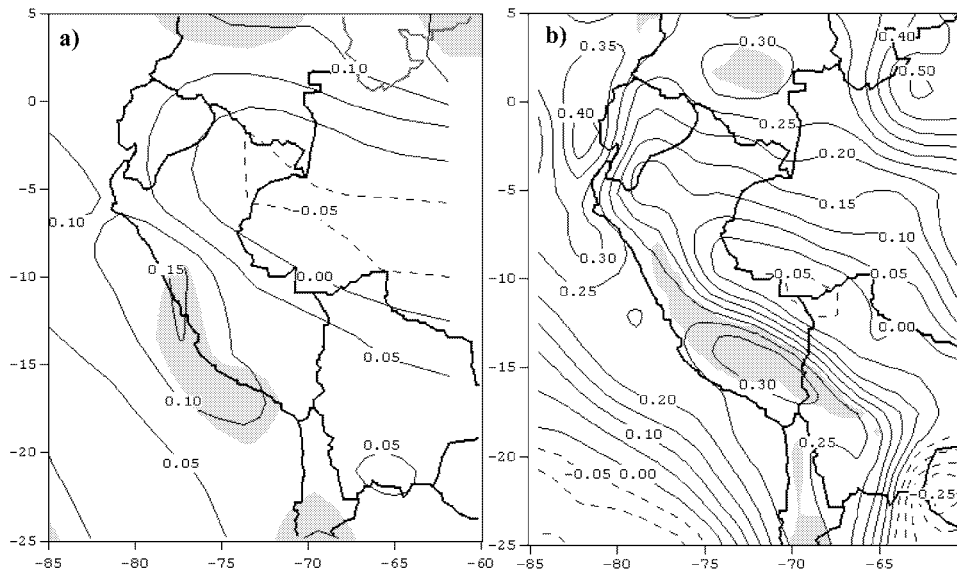


Figure 7. Temperature trend for (a) ECHAM-4 T30 (1950–1994), (b) ECHAM-4 T106 (1979–1998). Contour interval is $0.05^{\circ}\text{C decade}^{-1}$; negative contours are dashed. Regions where the trend is significantly increasing at the 95%-confidence level are shaded in gray. Figure 7b has been smoothed with a 3×3 averaging filter.

slight cooling along the eastern slope but the warming over the Andes is as strong as and more significant than that along the Pacific coast (Figure 7b). This becomes more evident when the trends are examined separately for 1000 m elevation zones, again subsampled to match the location of observational station records. Because the spatial resolution in the T30 simulation is too coarse to accurately represent the Andean topography we only show the results for the high-resolution simulation T106 (Figure 8a). Even though the time periods between observations (1959–1994) and the ECHAM-4 T106 model (1979–1998) are different, the vertical structure of the temperature trend in Figure 8a is remarkably similar to the observational results (Figure 5). The differential warming of the eastern and western slopes is clearly reproduced by the model even though the temperature increase below 2000 m on the Pacific side seems to be underestimated. The most notable differences between model and observations include the increased warming up to the highest elevations, not apparent in the two observational data sets and the generally stronger (although mostly insignificant) warming in the model, which can be attributed to the more recent time period over which the model was integrated (1979–1998).

The markedly different warming to the east and the west of the Andes is not restricted to near surface levels but apparent throughout the lower and middle model troposphere (Figure 9). Interestingly however, this feature is not apparent in all seasons but caused by a very strong east-west gradient in the trend in JJA. At this time of the year the warming is significant throughout the model troposphere

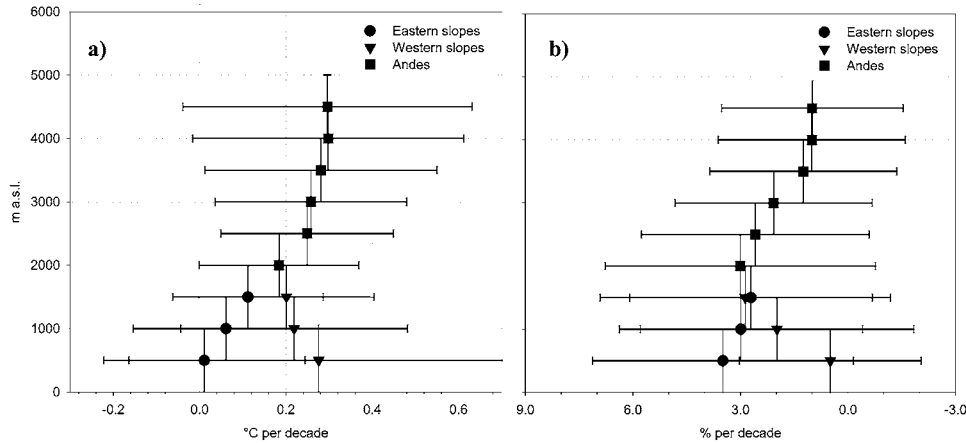


Figure 8. (a) Mean annual temperature trend ($^{\circ}\text{C decade}^{-1}$) as a function of elevation (m a.s.l.) based on ECHAM-4 T106 simulation (1979–1998). Vertical bars indicate elevation range (1000 m) for which trend is valid. Horizontal bars are 95% confidence limits for the trend (i.e., all trends whose error bars do not intersect with the $0^{\circ}\text{C decade}^{-1}$ abscissa are significant at the 95% confidence level). Results are based on sub-sampling to match station coverage in Figure 5a, that is only grid cells which contain station data in Figure 5a are considered. (b) as in (a) but for JJA total integrated cloud cover (in $\% \text{ decade}^{-1}$) in ECHAM-4 T106 simulation. Note that scale for x-axis is reversed in Figure 8b).

in both simulations to the west of the Andes, while to the east a cooling is apparent below ~ 850 hPa and the warming is less than to the west and insignificant throughout the entire troposphere (Figures 9c,f). We discuss potential causes for this markedly different trend to the east and the west of the Andes in JJA in the next section.

Figures 10a–c show the trend in relative humidity based on the ECHAM-4 T106 model experiment between 1979 and 1995, to facilitate comparison with the observational trend shown for the same time period in Figures 6d–f. The model results indicate a strong NE–SW gradient across the Andes. The NE part of the Andes show a modest increase in mean annual relative humidity ranging between 0 and $2.5\% \text{ decade}^{-1}$ over the last 20 years. Negative trends occur along the western Andean slope in southern Peru and northern Chile (Figure 6a). The general rising trend over most of the Andes is consistent with the observational results from the CRU05 data set (Figures 6d–f), but otherwise there is little resemblance between observations and model results. This is especially apparent to the east of the Andes, where the model simulates the largest increase in relative humidity (in particular during JJA, Figure 10c), while the trends in the observations are mostly negative. The model may not be able to accurately simulate the observed changes in relative humidity, but the humidity increase to the east of the Andes seems nonetheless more consistent with the observed increase in convection over a comparable time period (Figure 2a), or reports of increased specific humidity levels over the Amazon

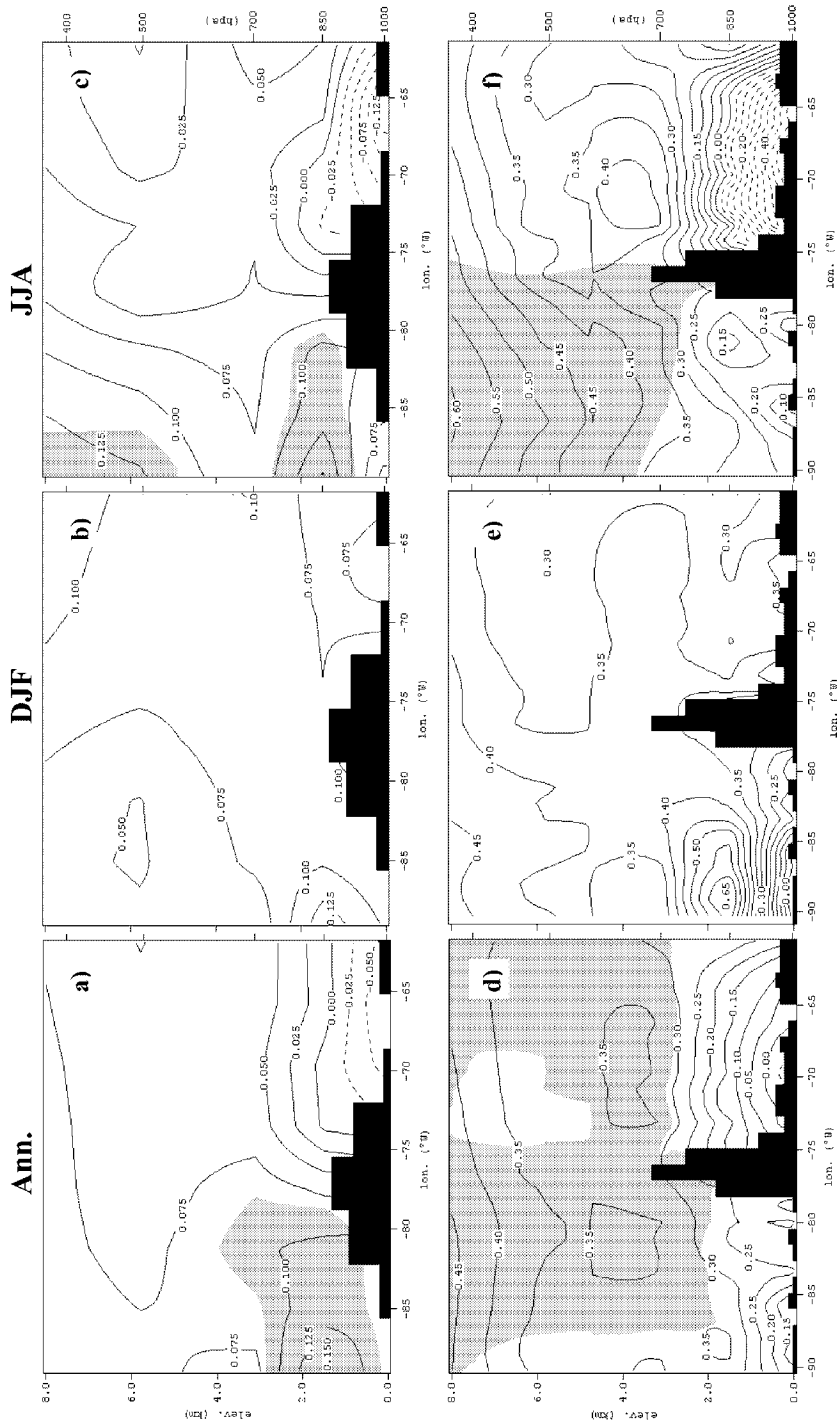


Figure 9. Tropospheric temperature trends (in $^{\circ}\text{C decade}^{-1}$) as a function of pressure level and longitude. Cross section shows zonal average from $\sim 0^{\circ}$ to 10°S across the tropical Andes from $\sim 90^{\circ}$ to 60°W . Figures are based on results from 250 hPa, 500 hPa, 700 hPa, 850 hPa and 1000 hPa levels and are interpolated in between. Top row: ECHAM-4 T30 (1950–1994); bottom row: ECHAM-4 T106 (1979–1998). Trends are shown for annual mean (left column), DJF (middle column) and JJA (right column). Contour interval is $0.025^{\circ}\text{C decade}^{-1}$ in (a)–(c) and $0.05^{\circ}\text{C decade}^{-1}$ in (d)–(f); negative contours are dashed. Significant trends at the 95% confidence level are shaded in gray. Black shaded areas represent model topography.

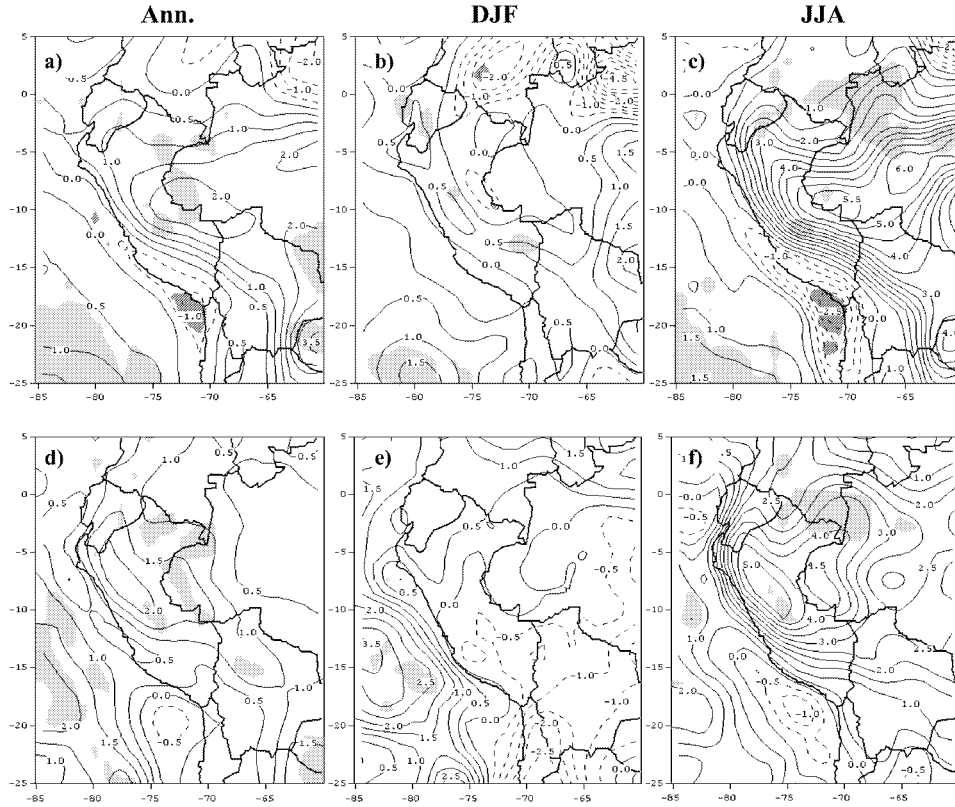


Figure 10. Trend in relative humidity (in $\% \text{ decade}^{-1}$, top row) between 1979 and 1995 and total cloud cover (in $\% \text{ decade}^{-1}$, bottom row) between 1979 and 1998 based on ECHAM-4 T106 simulation. Trends are shown for annual mean (left column), DJF (middle column) and JJA (right column). Contour interval is 0.5%, negative contours are dashed and regions where humidity or total cloud cover has significantly increased (decreased) at the 95% confidence level are shaded in light (dark) gray. Figures have been smoothed with a 3×3 averaging filter.

basin (e.g., Chen et al., 2001) than with the negative trends in the observational data.

4.2. TEMPERATURE TRENDS, CLOUD COVER AND TROPICAL SST

The reason for the differential trends along the eastern and western slopes is not clear, but worthy of further investigation. Since convective activity has increased over tropical South America to the east of the Andes (Figure 2), it is reasonable to assume that the markedly different temperature trends may be affected by changes in cloud cover as well. The observed increase in convective cloud cover to the east of the Andes may have dampened the near-surface warming through a reduction of incoming shortwave radiation, while this effect is probably of minor importance over the arid western slopes of the Andes. The east-west difference

in the temperature trend is most apparent in JJA (Figure 9), and indeed the largest increase in total cloud cover (in % decade⁻¹) has occurred in JJA (Figure 10f) and is located to the east of the Andes, where the cooling in the model is most pronounced (Figures 9c,f). This close relationship between cloud cover and temperature trends is even more apparent when the JJA change in total cloud cover is plotted versus elevation, subsampled the same way as for temperature in Figure 8. JJA cloud cover trends (Figure 8b) closely mirror the trends in annual temperature (Figure 8a). On the eastern slopes where temperature trends are the lowest, cloud cover has increased the most and vice-versa. The correlation between annual temperature and JJA cloud cover trends based on individual grid cells is -0.61 , significant at 99.9% level, if subsampled over the Andes. However, the simulated temperature trends are slightly positive everywhere, despite the general cloud cover increase. This indicates that cloud cover changes may have modified or dampened the observed warming trend in particular to the east of the Andes, but it does not explain the overall warming trend. These results however should be interpreted with caution because there is ample evidence suggesting that the correct model simulation of clouds is difficult (Trenberth, 2002). For example the simulated cloud cover increase in JJA (Figure 10f) is not apparent in the OLR data (Figure 2) although the general cloud cover increase is certainly consistent with the notion of enhanced convective activity in the inner tropics.

Since the general warming trend in the tropical Andes as well as the spatial pattern is correctly simulated by the ECHAM-model, and the model is only forced with observed global SST, it is plausible to assume that SST may play a role in the observed warming. The climate in the tropical Andes is closely related to SST in the central equatorial Pacific on interannual timescales, with both precipitation and temperature showing distinct departures from the mean during El Niño and La Niña events (e.g., Vuille, 1999; Vuille et al., 2000a,b, Garreaud and Aceituno, 2001; Garreaud et al., 2003). To further illustrate this relationship, the first Principal Component (PC #1) of temperature anomalies in the Andes of Ecuador (Figure 11a, Vuille et al., 2000a) and PC #1 of vapor pressure anomalies in the study area based on the CRU05 data (Figure 11b) are plotted against SSTA in the NINO4 region. Temperature and vapor pressure lag NINO4 SSTA by approximately 1 month, which indicates that they are forced by SSTA in the central equatorial Pacific. At the same time sea surface temperature has increased considerably in the tropical Pacific domain over the last decades (e.g., Casey and Cornillon, 2001). It is therefore reasonable to assume that the observed climate change in the tropical Andes may, at least in part, be caused by a concurrent change in the tropical Pacific. To further investigate this hypothesis and to see what fractions of the simulated warming trends are linearly congruent with a contemporaneous change in the tropical Pacific, we regressed simulated monthly near-surface temperature anomalies onto standardized monthly anomalies of the NINO4-index and then multiply the regression coefficients by the trend in the NINO4-index ($0.0021\text{ }^{\circ}\text{C month}^{-1}$ between 1979–1998). This yields an estimate of the fraction of the trend

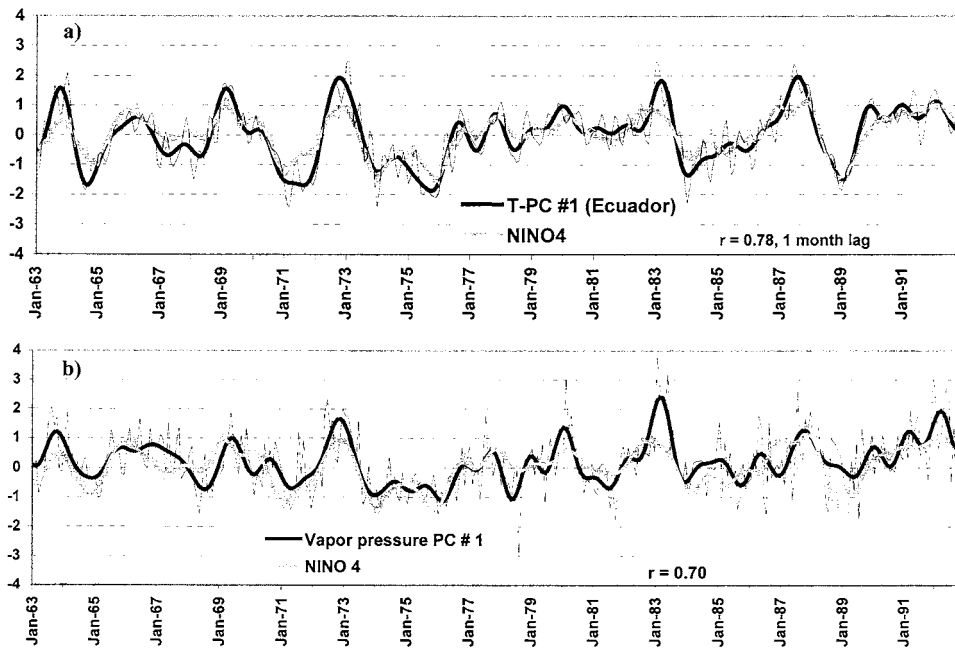


Figure 11. Correlation of NINO4-index with (a) PC #1 of Ecuadorian Andes temperature anomalies (Vuille et al., 2000a) between 1963 and 1992 and (b) PC #1 of tropical Andes vapor pressure anomalies (CRU05, 1963–1992). Thick lines are low pass-Hamming weights filtered.

which can be attributed solely to the warming in the NINO4 region. The signature of the NINO4-index (Figure 12b) is clearly reflected in both the spatial pattern and the sign of the simulated trend (Figure 12a). Roughly 50–70% of the simulated warming along the Pacific coast is linearly congruent with the trend in the NINO4 region and can be attributed to warming in the central equatorial Pacific. Similarly the cooling to the east of the Andes is not caused by the NINO4 trend alone, but clearly the linearly congruent trend is weakest in the same places where the simulation shows a negative trend. Hence the east-west difference in the simulated temperature trend can in part be attributed to the warming in the central equatorial Pacific. The strong simulated warming at high elevation in southern Peru ($>0.30\text{ }^{\circ}\text{C decade}^{-1}$) however, is a feature which does not seem to be strongly related to an increase in tropical SST.

5. Summary and Conclusions

Linear trend analysis of observational data and model diagnostics from an atmospheric general circulation model are used to search for potential mechanisms related to the observed glacier retreat in the tropical Andes between 1950 and 1998. Changes in precipitation amount or cloud cover are minor in most regions and

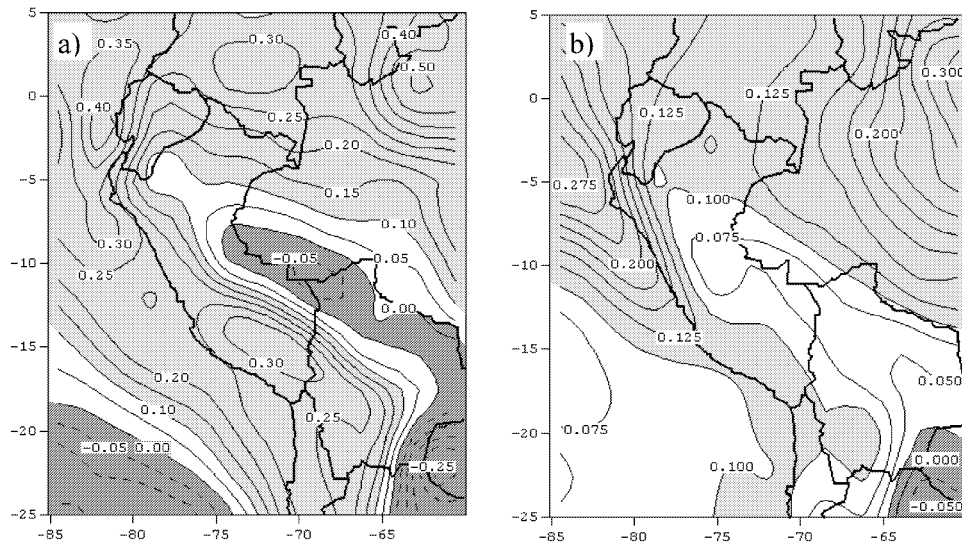


Figure 12. (a) Annual mean temperature trend (in $^{\circ}\text{C decade}^{-1}$) and (b) the contribution of the NINO4 index to the trend (in $^{\circ}\text{C decade}^{-1}$) in the ECHAM-4 T106 simulation between 1979 and 1998. Contour interval is $0.05^{\circ}\text{C decade}^{-1}$ in (a) and $0.025^{\circ}\text{C decade}^{-1}$ in (b); negative contours are dashed. Negative values are shaded in dark gray, values >0.1 are shaded in light gray. Figures have been smoothed with a 3×3 averaging filter.

it is therefore rather unlikely that these factors have caused the observed retreat. Near-surface temperature and humidity levels on the other hand have increased significantly throughout the tropical Andes, although long-term on-site measurements will be needed to validate the CRU 05 humidity data in the tropical Andes. The temperature increase varies markedly between the eastern and western Andean slopes with a much larger temperature increase to the west. Simulations with the ECHAM-4 model, forced with observed global sea surface temperatures (SST) realistically reproduce the observed warming trend as well as the spatial trend pattern. The increase in relative humidity is also apparent in the model simulations, but on a regional scale the results between model and observations vary significantly. Model results further suggest that a significant fraction of the observed warming as well as the spatially varying trend can be traced to a concurrent rise in SST in the equatorial Pacific. This is consistent with results from a modeling study by Diaz and Graham (1996), who showed that the observed changes in tropical freezing level heights are most likely caused by an increase in tropical SST. The model results further suggest that markedly different trends in cloud cover to the east and west of the Andes may have further modified this spatially varying trend across the Andes.

Recent observations from the Bolivian Andes suggest that humidity, which governs sublimation; precipitation, whose variability controls the albedo of the glacier and cloudiness, which controls the incoming long-wave radiation, may be more

important factors than temperature, to explain the observed mass loss of tropical glaciers (e.g., Wagnon et al., 2001). However, all these meteorological variables are strongly interconnected, and temperature, integrating all these fluxes, is significantly correlated with mass balance on time-scales of years and longer (Francou et al., 2003). Therefore, air temperature remains a relevant variable to explain glacier mass balance evolution and is a good indicator for climate change, which might affect long-term mass balance trends.

We emphasize that it is important to separate the general trend of receding glaciers from interannual glacier movement, which shows both phases of advance and recession. In this context it is noteworthy that the last two phases of glacier advances in the early 1970s and most recently since 1999 (G. Kaser, personal communication) both coincide with persistent cold La Niña conditions in the tropical Pacific. This behavior renders further support for the notion that tropical Andean glaciers are closely linked to the climate of the tropical Pacific, and react to SST changes that persist for a few years with a very short time-lag. The main reason for this close association is that the response to SSTA in the tropical Pacific is either a cold/wet (La Niña) or warm/dry (El Niño) signal in the Andes, but hardly ever is it warm/wet or cold/dry (Vuille, 1999; Vuille et al., 2000a,b). Thus the SST signal in the tropical Pacific is amplified over the tropical Andes in the sense that it shows a thermal and a hydrologic response, which both act in favor of (La Niña) or against (El Niño) a positive glacier mass balance.

An obvious limitation of this study is the lack of data for the first half of this century. The climatic trends shown in this study are limited to the last five decades and accordingly they can only explain the glacier retreat over this time interval. The initial glacier recession in the tropical Andes however started much earlier, in the second half of the 19th century, and its causes are unknown.

Despite the new insight into climate change issues in the tropical Andes that our study was able to provide, this kind of analysis cannot replace field programs with detailed energy and mass balance measurements. Such field studies are needed to improve our understanding of tropical glacier – climate relationships and should be expanded to monitor future changes in the tropical Andes.

Acknowledgements

This article greatly benefited from discussions with J. L. Betancourt, H. F. Diaz, D. R. Hardy, S. Hastenrath, G. Kaser, D. J. Seidel and L. G. Thompson. Brian Mark kindly contributed data from Peru that was used to update the temperature time series. The comments and suggestions by Vera Markgraf, Ricardo Villalba and an anonymous reviewer helped to significantly improve this manuscript. ECHAM simulations were performed with support of the German Climate Computing Centre (DKRZ) in Hamburg, Germany. ECT-corrected OLR data were provided by the National Center for Atmospheric Research – Data Support Section (NCAR-DSS).

CRU05 data were received from the Oak Ridge National Laboratory – Distributed Active Archive Center (ORNL-DAAC). This study was supported by US-NSF grant ATM-9909201 and by the U.S. Dept. of Energy.

References

- Aceituno, P. and Montecinos, A.: 1997, 'Patterns of Convective Cloudiness in South America during Austral Summer from OLR Pentads', in *Preprints, Fifth Int. Conf. on Southern Hemisphere Meteorology and Oceanography*, Pretoria, South Africa, *Amer. Meteor. Soc.*, 328–329.
- Ames, A. and Hastenrath, S.: 1996, 'Mass Balance and Ice Flow of the Uirashraju Glacier, Cordilera Blanca, Peru', *Zeitschrift für Gletscherkunde und Glazialgeologie* **32**, 83–89.
- Ames, A.: 1998, 'A Documentation of Glacier Tongue Variations and Lake Development in the Cordillera Blanca, Peru', *Zeitschrift für Gletscherkunde und Glazialgeologie* **34**, 1–36.
- Brecher, H. H. and Thompson, L. G.: 1993, 'Measurement of the Retreat of Qori Kalis Glacier in the Tropical Andes of Peru by Terrestrial Photogrammetry', *Photogramm. Eng. Rem. Sens.* **59**, 1017–1022.
- Casey, K. S. and Cornillon, P.: 2001, 'Global and Regional Sea Surface Temperature Trends', *J. Climate* **14**, 3801–3818.
- Chen, J., Carlson, B. E., and Del Genio, A. D.: 2002, 'Evidence for Strengthening of the Tropical General Circulation in the 1990s', *Science* **295**, 838–841.
- Chen, T.-C., Yoon, J. H., St. Croix, K. J., and Takle, E. S.: 2001, 'Suppressing Impacts of the Amazonian Deforestation by the Global Circulation Change', *Bull. Amer. Meteorol. Soc.* **82**, 2209–2216.
- Chu, P.-S., Yu, Z.-P., and Hastenrath, S.: 1994, 'Detecting Climate Change Concurrent with Deforestation in the Amazon Basin: Which Way Has It Gone?', *Bull. Amer. Meteorol. Soc.* **75**, 579–583.
- Curtis, S. and Hastenrath, S.: 1999a, 'Long-term Trends and Forcing Mechanisms of Circulation and Climate in the Equatorial Pacific', *J. Climate* **12**, 1134–1144.
- Curtis, S. and Hastenrath, S.: 1999b, 'Trends of Upper-air Circulation and Water Vapour over Equatorial South America and Adjacent Oceans', *Int. J. Clim.* **19**, 863–876.
- Diaz, H. F. and Graham, N. E.: 1996, 'Recent Changes in Tropical Freezing Heights and the Role of Sea Surface Temperature', *Nature* **383**, 152–155.
- Francou, B., Ramirez, E., Caceres, B., and Mendoza, J.: 2000, 'Glacier Evolution in the Tropical Andes during the Last Decades of the 20th Century: Chacaltaya, Bolivia and Antizana, Ecuador', *Ambio* **29**, 416–422.
- Francou, B., Vuille, M., Wagnon, P., Mendoza J., and Sicart, J. E.: 2003, 'Tropical Climate Change Recorded by a Glacier in the Central Andes during the Last Decades of the 20th Century: Chacaltaya, Bolivia, 16° S', *J. Geophys. Res.* **108** D5, 4154, doi: 10.1029/2002JD002959.
- Gaffen, D. J., Santer, B. D., Boyle, J. S., Christy, J. R., Graham, N. E., and Ross, R. J.: 2000, 'Multidecadal Changes in the Vertical Temperature Structure of the Tropical Troposphere', *Science* **287**, 1242–1245.
- Garreaud, R. and Aceituno, P.: 2001, 'Interannual Rainfall Variability over the South American Altiplano', *J. Climate* **14**, 2779–2789.
- Garreaud, R., Vuille, M., and Clement, A.: 2003, 'The Climate of the Altiplano: Observed Current Conditions and Mechanisms of Past Changes', *Palaeogeogr. Palaeoclimatol. Palaeoecol.* **194**, 5–22.
- Gutzler, D. S.: 1992, 'Climatic Variability of Temperature and Humidity over the Tropical Western Pacific', *Geophys. Res. Lett.* **19**, 1595–1598.
- Hastenrath, S. and Kruss, P. D.: 1992a, 'Greenhouse Indicators in Kenya', *Nature* **355**, 503–504.

- Hastenrath, S. and Kruss, P. D.: 1992b, 'The Dramatic Retreat of Mount Kenya's Glaciers between 1963 and 1987: Greenhouse Forcing', *Ann. Glaciol.* **16**, 127–133.
- Hastenrath, S. and Ames, A.: 1995, 'Diagnosing the Imbalance of Yanamarey Glacier in the Cordillera Blanca of Peru', *J. Geophys. Res.* **100**, 5105–5112.
- Hastenrath, S.: 2001, 'Variations of East African Climate during the Past Two Centuries', *Clim. Change* **50**, 209–217.
- Kaser, G. and Georges, C.: 1997, 'Changes of the Equilibrium-line Altitude in the Tropical Cordillera Blanca, Peru, 1930–1950, and their Spatial Variations', *Ann. Glaciol.* **24**, 344–349.
- Kaser, G.: 1999, 'A Review of the Modern Fluctuations of Tropical Glaciers', *Global Planet. Change* **22**, 93–103.
- Kaser, G. and Georges, C.: 1999, 'On the Mass Balance of Low Latitude Glaciers with Particular Consideration of the Peruvian Cordillera Blanca', *Geogr. Ann.* **81A**, 643–651.
- Kousky, V. E. and Kayano, M. T.: 1994, 'Principal Modes of Outgoing Longwave Radiation and 250 mb Circulation for the South American Sector', *J. Climate* **7**, 1131–1143.
- Liebmann, B., Marengo, J. A., Glick, J. D., Kousky, V. E., Wainer, I. C., and Massambani, O.: 1998, 'A Comparison of Rainfall, Outgoing Longwave Radiation and Divergence over the Amazon Basin', *J. Climate* **11**, 2898–2909.
- Liu, X. and Chen, B.: 2000, 'Climatic Warming in the Tibetan Plateau during Recent Decades', *Int. J. Clim.* **20**, 1729–1742.
- Lucas, L. E., Waliser, D. E., Xie, P., Janowiak, J. E., and Liebmann, B.: 2001, 'Estimating the Satellite Equatorial Crossing Time Biases in the Daily, Global Outgoing Longwave Radiation Dataset', *J. Climate* **14**, 2583–2605.
- Morrissey, M. L.: 1986, 'A Statistical Analysis of the Relationships among Rainfall, Outgoing Longwave Radiation and the Moisture Budget during January–March 1979', *Mon. Wea. Rev.* **114**, 931–942.
- Morrissey, M. L. and Graham, N. E.: 1996, 'Recent Trends in Rain Gauge Precipitation Measurements from the Tropical Pacific: Evidence for an Enhanced Hydrologic Cycle', *Bull. Amer. Meteorol. Soc.* **77**, 1207–1219.
- New, M., Hulme, M., and Jones, P.: 2000, 'Representing Twentieth-century Space-time Climate Variability. Part II: Development of 1901–1996 Monthly Grids of Terrestrial Surface Climate', *J. Climate* **13**, 2217–2238.
- Peterson, T. C., Karl, T. R., Jamason, P. F., Knight, R., and Easterling, D. R.: 1998, 'First Difference Method: Maximizing Station Density for the Calculation of Long-term Global Temperature Change', *J. Geophys. Res.* **103**, 25967–25974.
- Quintana-Gomez, R. A.: 1999, 'Trends of Maximum and Minimum Temperatures in Northern South America', *J. Climate* **12**, 2104–2112.
- Ramirez, E., Francou, B., Ribstein, P., Desclitres, M., Guerin, R., Mendoza, J., Gallaire, R., Pouyaud, B., and Jordan, E.: 2001, 'Small Glaciers Disappearing in the Tropical Andes: A Case Study in Bolivia: Glaciar Chacaltaya (16° S)', *J. Glaciol.* **47**, 187–194.
- Ribstein, P., Tiriau, E., Francou, B., and Saravia, R.: 1995, 'Tropical Climate and Glacier Hydrology: A Case Study in Bolivia', *J. Hydrol.* **165**, 221–234.
- Ronchail, J.: 1995, 'Variabilidad interanual de las precipitaciones en Bolivia', *Bull. Inst. fr. études andines* **24**, 369–378.
- Rosenblüth, B., Fuenzalida, H. A., and Aceituno, P.: 1997, 'Recent Temperature Variations in Southern South America', *Int. J. Clim.* **17**, 67–85.
- Rossow, W. B. and Schiffer, R. A.: 1999, 'Advances in Understanding Clouds from ISCCP', *Bull. Amer. Meteorol. Soc.* **80**, 2261–2287.
- Thompson, L. G.: 2000, 'Ice Core Evidence for Climate Change in the Tropics: Implications for Our Future', *Quat. Sci. Rev.* **19**, 19–35.
- Trenberth, K. E.: 2002, 'Changes in Tropical Clouds and Radiation', *Science* **296**, 2095a.

- Villalba, R., Grau, H. R., Boninsegna, J. A., Jacoby, G. C., and Ripalta, A.: 1998, 'Tree-ring Evidence for Long-term Precipitation Changes in Subtropical South America', *Int. J. Clim.* **18**, 1463–1478.
- Vuille, M.: 1999, 'Atmospheric Circulation over the Bolivian Altiplano during DRY and WET Periods and Extreme Phases of the Southern Oscillation', *Int. J. Clim.* **19**, 1579–1600.
- Vuille, M. and Bradley, R. S.: 2000, 'Mean Annual Temperature Trends and their Vertical Structure in the Tropical Andes', *Geophys. Res. Lett.* **27**, 3885–3888.
- Vuille, M., Bradley, R. S., and Keimig, F.: 2000a, 'Climatic Variability in the Andes of Ecuador and its Relation to Tropical Pacific and Atlantic Sea Surface Temperature Anomalies', *J. Climate* **13**, 2520–2535.
- Vuille, M., Bradley, R. S., and Keimig, F.: 2000b, 'Interannual Climate Variability in the Central Andes and its Relation to Tropical Pacific and Atlantic Forcing', *J. Geophys. Res.* **105**, 12447–12460.
- Vuille, M., Bradley, R. S., Werner, M., Healy, R., and Keimig, F.: 2003a, 'Modeling $\delta^{18}\text{O}$ in Precipitation over the Tropical Americas, I: Interannual Variability and Climatic Controls', *J. Geophys. Res.* **108** D6, 4174, doi: 10.1029/2001JD002038.
- Vuille, M., Bradley, R. S., Healy, R., Werner, M., Hardy, D. R., Thompson, L. G., and Keimig, F.: 2003b, 'Modeling $\delta^{18}\text{O}$ in Precipitation over the Tropical Americas, II: Simulation of the Stable Isotope Signal in Andean Ice Cores', *J. Geophys. Res.* **108** D6, 4174, doi: 10.1029/2001JD002039.
- Wagon, P., Ribstein, P., Francou, B., and Pouyaud, B.: 1999a, 'Annual Cycle of Energy Balance of Zongo Glacier, Cordillera Real, Bolivia', *J. Geophys. Res.* **104**, 3907–3923.
- Wagon, P., Ribstein, P., Kaser, G., and Berton, P.: 1999b, 'Energy Balance and Runoff Seasonality of a Bolivian Glacier', *Glob. Plan. Change* **22**, 49–58.
- Wagon, P., Ribstein, P., Francou, B., and Sicart, J. E.: 2001, 'Anomalous Heat and Mass Budget of Glacier Zongo, Bolivia, during the 1997–98 El Niño Year', *J. Glaciol.* **47**, 21–28.
- Waliser, D. E., Graham, N. E., and Gautier, C.: 1993, 'Comparison of the Highly Reflective Cloud and Outgoing Longwave Radiation Data Sets for Use in Estimating Tropical Deep Convection', *J. Climate* **6**, 331–353.
- Waliser, D. E. and Zhou, W. F.: 1997, 'Removing Satellite Equatorial Crossing Time Biases from the OLR and HRC Datasets', *J. Climate* **10**, 2125–2146.
- Weatherhead, E. C., Reinsel, G. C., Tiao, G. C., Meng, X. L., Choi, D., Cheang, W. K., Keller, T., DeLuise, J., Wuebbles, D. J., Kerr, J. B., Miller, A. J., Oltmans, S. J., and Frederick, J. E.: 1998, 'Factors Affecting the Detection of Trends: Statistical Considerations and Applications to Environmental Data', *J. Geophys. Res.* **103**, 17149–17161.
- Wielicki, B. A., Wong, T., Allan, R. P., Slingo, A., Kiehl, J. T., Soden, B. J., Gordon, C. T., Miller, A. J., Yang, S. K., Randall, D. A., Robertson, F., Susskind, J., and Jacobowitz, H.: 2002, 'Evidence for Large Decadal Variability in the Tropical Mean Radiative Energy Budget', *Science* **295**, 841–844.

(Received 19 September 2001; in revised form 18 December 2002)